Tellus (1983), *35A*, 88–99

Spectral study of wintertime kinetic energy of the northern hemisphere in the troposphere

By H. N. LEE, Z. ZHAO* and S. K. KAO**, *Department of Meteorology, University of Utah, Salt Lake City, Utah 84112, U.S.A.*

(Manuscript received September 10, 1981; in final form April 5, 1982)

ABSTRACT

The regional distribution of kinetic energy has been computed and analyzed in a wave number-frequency domain at 850 mb, 500 mb and 200 mb. The distribution of kinetic energy shows a strong geographic dependence. It is found that medium scale (wave number between 6 and 9) westerly waves with medium frequency (period between 3 days and 9 days) significantly contribute to the 2 distinctive kinetic energy maxima located over the North Pacific and the east coast of North America. Easterly waves with medium and high frequency have no substantial contribution.

An analysis of the effects of non-linear interactions on the regional distribution and characteristics of the kinetic energy of the medium scale westerly waves with medium frequency indicates that the contribution of non-linear interactions corresponding to the longitudinal convergence of the flux of kinetic energy is generally larger than that of the terms involving the meridional convergence of the flux of kinetic energy. The primary non-linear interactions occur at mid-latitudes between 30° N and 50° N. The regions at 200 mb (500 mb) located to the north (south) of the maximum intensity of kinetic energy over the North Pacific are characterized by a negative contribution from non-linear interactions. The analysis reveals that the distribution of maximum intensity of kinetic energy over the North Pacific is positively correlated with the distribution of the non-linear interaction contribution. It indicates that non-linear interactions play an important rôle in the dynamics of atmospheric waves.

1. Introduction

The energetics of large-scale atmospheric waves is of vital importance in atmospheric phenomena. Considerable research has been done on the characteristics and energetics of large-scale atmospheric waves (e.g. Wiin-Nielsen, 1976; Kao, 1968, 1980; Wendell, 1969; Kao and Wendell, 1970; Steinberg *et al.*, 1971; Gruber, 1975; Tenenbaum, 1976; Burrows, 1976; Kao and Lee, 1977). However, these studies have been mostly confined to global distributions and to characteristics of the seasonal or annual mean state of the waves. In view of the effects of the distribution of continents and oceans, the characteristics of wave energy are affected by regional differences in the structure of the atmospheric waves. Relatively little attention has been devoted to investigating these. It is felt that to properly understand the characteristics of atmospheric waves and to gain a deeper insight into the mechanism for the large-scale waves in the atmosphere, it is necessary to analyze the wave energy and the processes of non-linear interaction in the wave number–frequency domain.

Recently the regional characteristics of the observed Northern Hemisphere wintertime circulation have been examined (Blackmon, 1976; Blackmon *et al.*, 1977, 1979; Lau, 1978, 1979; Blackmon and Lau, 1980). It was found that the regional features of the transient waves exhibited a strong relation to the distributions of continents and oceans. These studies were directed toward an understanding of the geographical distributions of temporal variance and covariance. Blackmon (1976)

*On leave from Central Weather Bureau, Peking, Peoples Republic of China.

** Deceased.

0280-6495/83/020088-12$02.50/0

showed that the temporal variability of the 500 mb geopotential height field, partitioned into different spatial scales and frequency bands, bore a strong geographical dependence. The medium frequency fields received substantial contributions from waves of synoptic scale at mid-latitudes. In this paper, we attempt to analyze the characteristics of the kinetic energy of wind fields at various pressure levels and to identify the relatively important waves in the wave number–frequency domain.

The studies presented by Lau (1979) on the diagnosis of local, time-averaged budgets of time-mean and transient eddy kinetic energy at 300 mb provide valuable information on the balance of kinetic energy through various types of interactions between the eddies and the time mean flow. The results are insufficient for an analysis of the mechanism of large-scale waves in the atmosphere. For example, how important is the non-linear interaction in a combined wave number–frequency domain? Which waves associated with which frequency imbedded in the non-linear interactions are of relative importance in regional contributions? What is the regional behaviour of non-linear interactions at the various pressure levels? In this paper, we intend to seek the answers to these important questions. The procedure is to use the Fourier transformed governing equations which have been considered as one of the fruitful approaches for the study of large-scale wave motions. We analyze the non-linear interaction terms of the kinetic energy equation in the wave number–frequency domain and examine the regional differences of non-linear interactions at various pressure levels in order to understand the important rôle of non-linear interactions in the transfer of kinetic energy in wave motions.

2. Data set and wave number–frequency technique

The data used in this study are the twice-daily NMC analyses of the wind fields at 850 mb, 500 mb and 200 mb which are available from the data archives of the National Center for Atmospheric Research. The 5° latitude–longitude square is the basic grid employed in this analysis. The analysis covered the region from 20° N to 60° N at 500 mb and from 20° N to 85° N at 200 mb and 850 mb. In this study we used data from the winter season 1 December 1975 to 1 March 1976.

Let $Q(k, n)$ be the complex Fourier coefficient of an atmospheric variable $q(\lambda, t')$ which is a function of longitude λ and time t', where k and n stand for wave number and frequency, respectively. The $q(\lambda, t)$ has a Fourier transform with respect to longitude λ and time t which may be written as

$$Q(k, n) = \frac{1}{4\pi^2} \int_0^{2\pi} \int_0^{2\pi} q(\lambda, t) e^{-i(k\lambda + nt)} d\lambda dt, \quad (1)$$

where $t = (2\pi/T)t'$ is a normalized period. The inverse transform of (1) gives $q(\lambda, t)$, expressed in terms of its Fourier coefficients as follows

$$q(\lambda, t) = \sum_{k=-\infty}^{\infty} \int_{-\infty}^{\infty} Q(k, n)\, e^{i(k\lambda + nt)}\, dn. \quad (2)$$

Here the summation of the Fourier coefficient Q with respect to the integer wave number is the consequence of the cyclic distribution of $q(\lambda, t)$ along latitude circles. The positive frequency sign represents the waves travelling westward and the negative sign eastward travelling waves.

Consider the same conditions for another variable $p(\lambda, t)$ with a Fourier transform $P(k, n)$. It can be shown that for variable $p(\lambda, t)$ and $q(\lambda, t)$ we have

$$\overline{p(\lambda, t)\, q(\lambda, t)} = \sum_{k=-\infty}^{\infty} \sum_{j=-\infty}^{\infty} \int_{-\infty}^{\infty} P(j, n)\, Q(k-j, -n)\, e^{ik\lambda}\, dn, \quad (3)$$

where the overbar denotes time-mean. Similarly, we have

$$\overline{p(\lambda, t)\, q(\lambda, t)\, r(\lambda, t)} = \sum_{k=-\infty}^{\infty} \sum_{j=-\infty}^{\infty} \sum_{L=-\infty}^{\infty} \int_{-\infty}^{\infty} \int_{-\infty}^{\infty} P(j, \omega)\, Q(L, \alpha) \times R(k-j-L, -\omega-\alpha)\, e^{il\lambda}\, d\omega d\alpha, \quad (4)$$

where $R(k, n)$ is a Fourier transform of $r(\lambda, t)$.

The complete truncated atmospheric variable and its covariance and variance can be recovered using (2)–(4). However, to investigate the characteristics of wave energy and the contributions from non-linear interactions it is appropriate to construct fields corresponding to summations over only part of the wave number and frequency. In this paper, we divided the wave number–frequency space into particular domains as shown in Tables 1 and 2. From the classification, according to wave number and frequency, it may be noted that there are 28 domains. Each domain is designated by combining the symbols used for the wave number and frequency classifications. For example, the domain of medium scale westerly waves with medium frequency would be represented by $(k_m, -n_m)$. The interaction combinations are designated by placing the category symbols side by side, e.g. $(k_m, -n_m)\,(k_L, n_m)$.

By using the formula (3), the kinetic energy may be computed as

$$\bar{E}(\lambda) = \tfrac{1}{2} \sum_{k=-\infty}^{\infty} \sum_{j=-\infty}^{\infty} \int_{-\infty}^{\infty} [U(k,n)\,U(k-j,-n) + V(k,n)\,V(k-j,-n)]\,e^{ik\lambda}\,dn, \qquad (5)$$

where $U(k, n)$ and $V(k, n)$ are the Fourier coefficients for the winds $u(\lambda, t)$ and $v(\lambda, t)$ respectively. It may be noticed that the waves in a certain domain $(k_L, \pm n_m)$ would contribute to the kinetic energy $\bar{E}(\lambda)$.

3. Regional distributions and characteristics of kinetic energy at 500 mb

Fig. 1 shows the regional distribution of kinetic energy composed of all wave scales at various frequencies. In Fig. 1a we see the total kinetic energy composed of all wave scales and all frequencies. 2 areas with maximum kinetic energy are seen. One begins at the east coast of Asia and extends all the way across the North Pacific. The other begins at the east coast of North America and extends across the North Atlantic. In Fig. 1b, it is found that the westerly waves with low frequency make contributions to the areas at the east coast of Asia, the west coast of America and north of central Europe. On the other hand, the easterly waves with low frequency (Fig. 1c) give contributions to kinetic energy east of the North Pacific and the North Atlantic. Figs 1d, e show the distributions of kinetic energy due to waves with medium frequency. We see from Fig. 1d that over the North Pacific and the east coast of North America, westerly waves with medium frequency dominate; this will be discussed in detail later. The intensity over the east coast of North America is stronger than over the North Pacific. The elongated cell over the North Pacific is oriented in an east-west direction. The easterly waves with medium frequency in Fig. 1e give no significant contribution. In all analyses, no substantial contributions are seen for high frequency waves.

It was noted by Blackmon (1976) that the elongated maxima extending across much of the North Pacific and Atlantic in the distribution of bandpass* variance of geopotential height could be identified with the major storm tracks and medium scale waves (wave number 7 to 12), and contributed substantially to the bandpass variance. In Fig. 2 we have plotted the contribution from

Table 1. *Wavenumber partition*

Wave number k	Classification	Symbol
0	Zonally averaged flow	0
1–5	Long (planetary) scale waves	k_L
6–9	Medium (synoptic) scale waves	k_m
10–36	Short scale waves	k_s

Table 2. *Frequency partition*

Frequency n (cycles per 90 days)	Period (days)	Classification (frequency)	Direction of wave motion	Symbol
−45 to −31	2–3	High	West to east	$-n_h$
−30 to −11	3–9	Medium	West to east	$-n_m$
−10 to −1	9–90	Low	West to east	$-n_L$
0		Zero	Stationary	0
1 to 10	9–90	Low	East to west	$+n_L$
11 to 30	3–9	Medium	East to west	$+n_m$
31 to 45	2–3	High	East to west	$+n_h$

* Period between 3 and 7 days which is closed to the period of medium frequency (between 3 and 9 days).

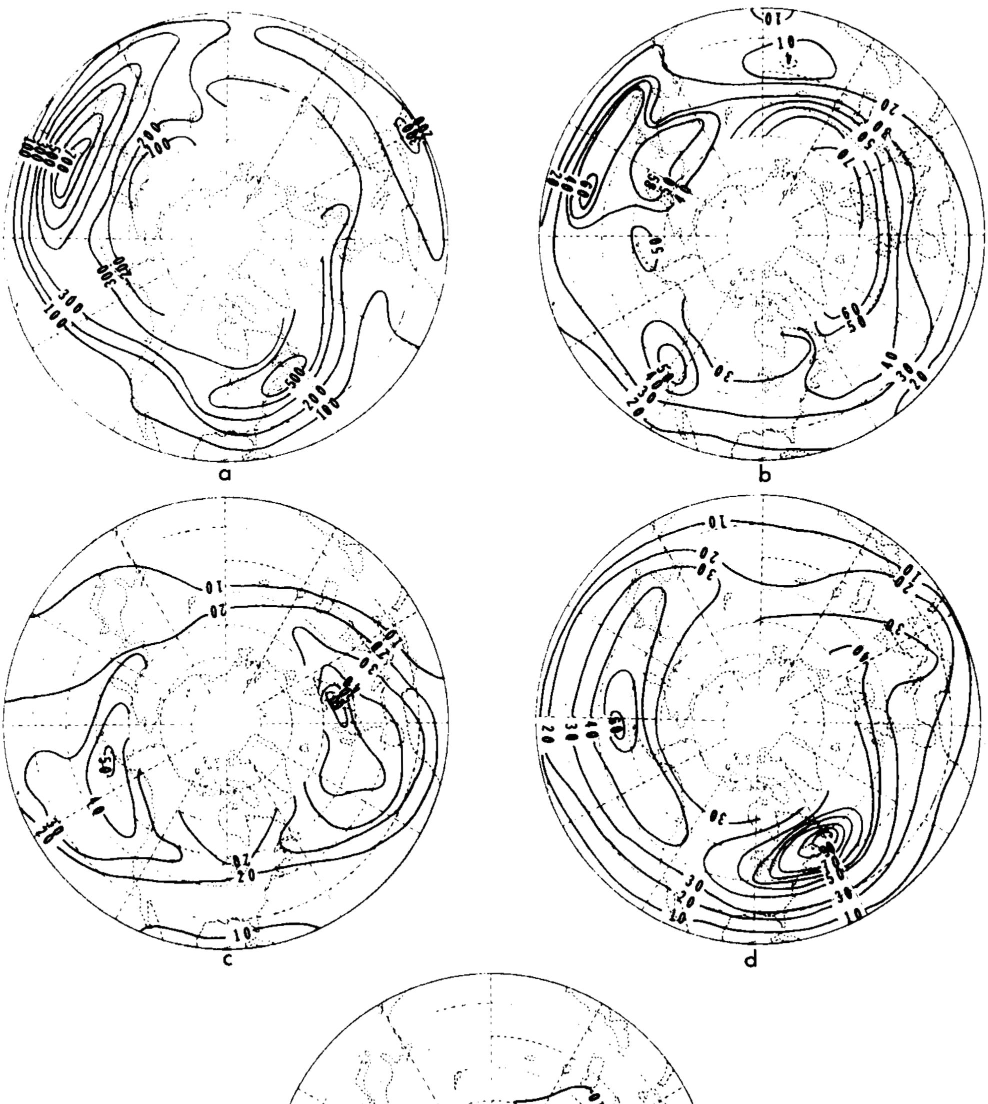

Fig. 1. Regional distributions of kinetic energy at 500 mb (units: $m^2 s^{-2}$). (a) All wave scales and all frequencies; (b) westerly waves with low frequency; (c) easterly waves with low frequency; (d) westerly waves with medium frequency; (e) easterly waves with medium frequency.

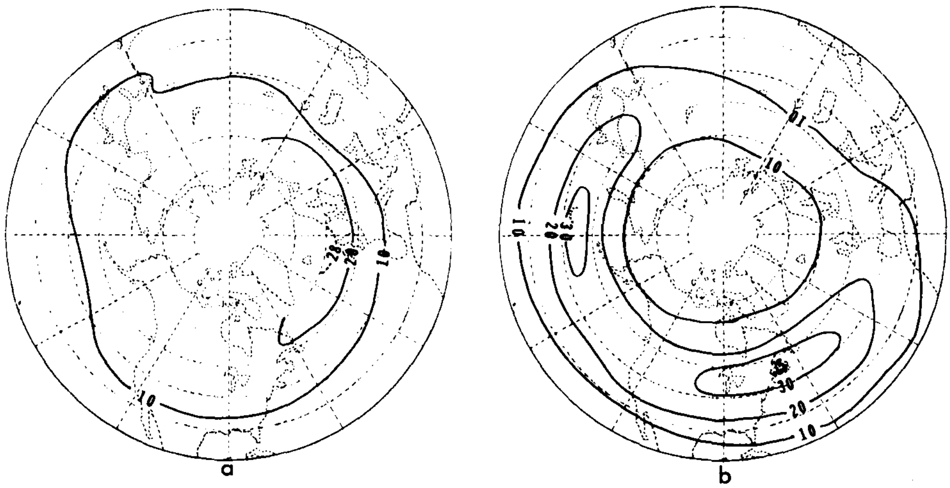

Fig. 2. Regional distributions of kinetic energy at 500 mb (units: $m^2 s^{-2}$). (a) Planetary scale westerly waves with medium frequency; (b) medium scale westerly waves with medium frequency.

planetary scale and medium scale westerly waves to the regional distributions of kinetic energy. In Fig. 2a it is seen that the planetary scale westerly waves with medium frequency seem to be responsible for the maximum at high latitudes over the east Atlantic. The short-scale westerly waves with medium frequency (not shown) make no contribution. However, the maximum kinetic energy over the North Pacific and the east coast of North America receive significant contributions from the medium scale westerly waves with medium frequency (Fig. 2b). This indicates the importance of medium-scale waves with medium frequency which are also found in the geopotential height analyses by Blackmon (1976). Here, the direction of propagation of medium-scale waves with medium frequency is identified. In the following sections we will investigate how these medium-scale westerly waves with medium frequency are maintained through non-linear interactions.

4. Regional distributions and characteristics of kinetic energy at 200 mb

The results for the distributions of kinetic energy at 200 mb are quite similar to those at 500 mb. Accordingly, some of the results will not be shown in this section. Fig. 3 shows the kinetic energy fields due to the waves with medium frequency. Fig. 3a shows the kinetic energy composed of all scales of westerly waves with medium frequency. In conformity with the 500 mb level there are 2 maxima. Comparing Figs. 3a and 1d, it is found that the tilt of the maximum kinetic energy with increasing altitude in the region of the North Pacific is marked, while the one in the east coast of North America is slight. Similarly, the maximum located over the east coast of North America appears stronger in comparison with that over the North Pacific. There are no significant contributions from the easterly waves with medium frequency (not shown). If we display the regional distributions of kinetic energy by wave number in the regime of westerly waves with medium frequency, we see that maximum contributions of planetary westerly waves with medium frequency are located over the North Atlantic at high latitudes (not shown) and the medium scale westerly waves with medium frequency give substantial contributions to the 2 distinctive maxima over the North Pacific and the east coast of North America (Fig. 3b).

In addition, Fig. 4 shows the kinetic energy of stationary waves. 3 regions of maximum kinetic energy are recognized: (1) over the east coast of Asia, (2) over eastern America and (3) over the North African continent. The intensity of the maximum in the east coast of Asia is much greater than that in eastern America. Fig. 5 shows the kinetic energy of transient eddies. These distributions of kinetic energy of stationary and tran-

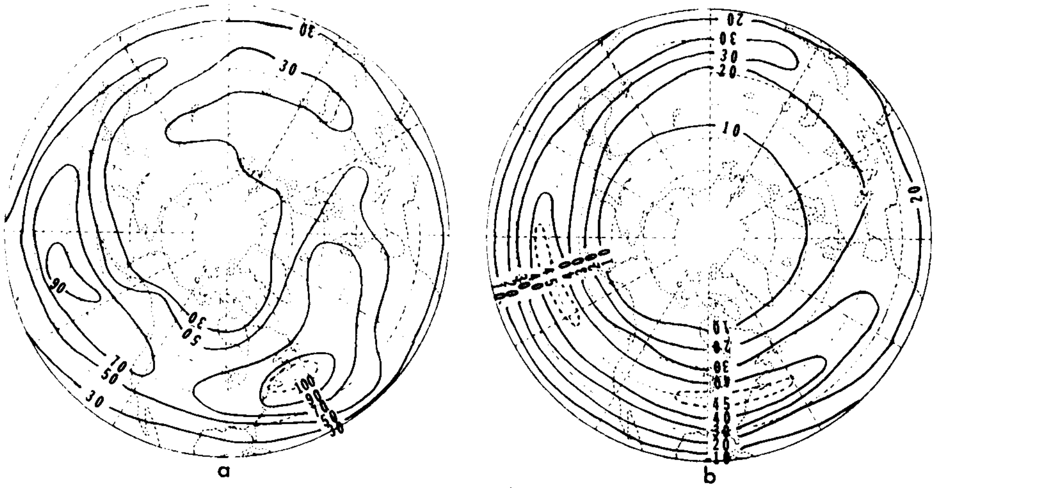

Fig. 3. Regional distributions of kinetic energy at 200 mb (units: $m^2 s^{-2}$). (a) Westerly waves with medium frequency; (b) medium scale westerly waves with medium frequency.

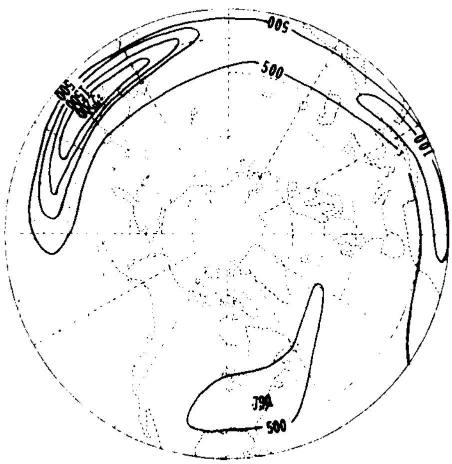

Fig. 4. Regional distribution of kinetic energy of stationary waves at 200 mb (units: $m^2 s^{-2}$).

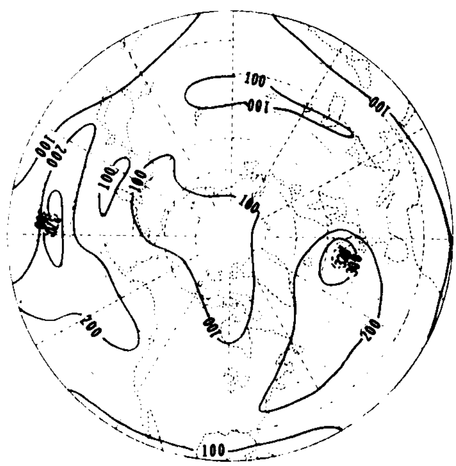

Fig. 5. As in Fig. 4 except for transient eddies.

sient flow are consistent with the results presented by Kao and Taylor (1964).

5. Regional distributions and characteristics of kinetic energy at 850 mb

Fig. 6 shows the distribution of kinetic energy of westerly waves with medium frequency. In Fig. 6a we see the kinetic energy composed of all scales of westerly waves. The patterns are similar and the maximum appears weak in comparison with Figs. 1d and 3a. Fig. 6a shows the contributions from the medium scale westerly waves with medium frequency. Comparing Fig. 6b with Figs. 2b and 3b, the tilt of maximum kinetic energy with increasing height in the region of the North Pacific is obvious.

6. Time-mean kinetic energy equation

In order to analyze the effects of non-linear interactions on the regional distributions and characteristics of the kinetic energy, the time-mean

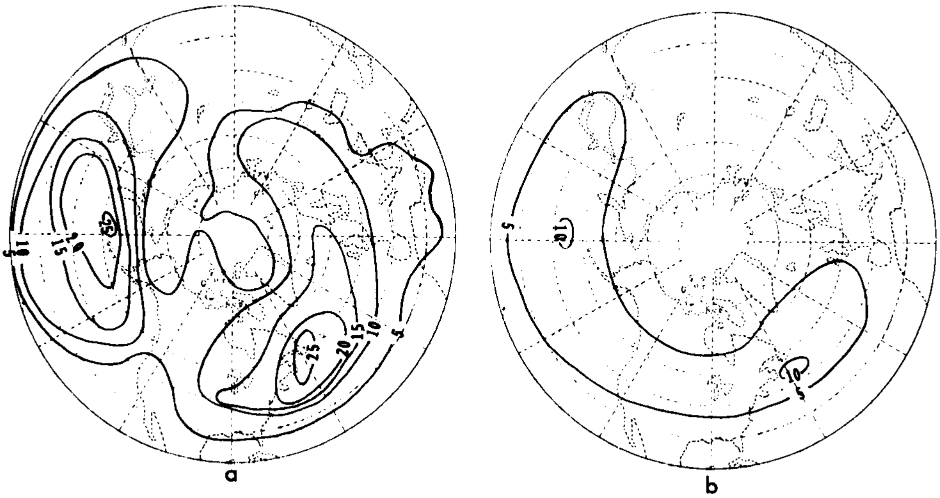

Fig. 6. Regional distributions of kinetic energy at 850 mb (units m² s⁻²). (a) Westerly waves with medium frequency; (b) medium scale westerly waves with medium frequency.

kinetic energy equation of the motion is considered. It may be expressed as

$$\frac{\partial \bar{E}(\lambda, t)}{\partial t} = -\frac{1}{a\cos\phi}\left(\overline{u^2\frac{\partial u}{\partial \lambda}} + \overline{uv\frac{\partial v}{\partial \lambda}}\right) - \frac{1}{a}\left(\overline{uv\frac{\partial u}{\partial \phi}} + \overline{v^2\frac{\partial v}{\partial \phi}}\right) - \left(\overline{uw\frac{\partial u}{\partial p}} + \overline{vw\frac{\partial v}{\partial p}}\right) + f(\overline{uv}_{\rm ag} - \overline{uv}_{\rm ag}) + \overline{uF}_1 + \overline{vF}_2, \quad (6)$$

where overbars denote time-mean, the subscript ag refers to ageostrophic wind components, λ is longitude, ϕ latitude, a earth radius, p pressure, F_1 and F_2 are components of the sum of the molecular and Reynolds stress forces, $\bar{E} = \frac{1}{2}(\overline{u^2} + \overline{v^2})$ is the kinetic energy.

To calculate the terms on the right-hand side of equation (6), we follow the procedures outlined in Section 2. For example, $\overline{uv\,\partial u/\partial\phi}$ is written as

$$\overline{uv\frac{\partial u}{\partial \phi}} = \sum_{k=-\infty}^{\infty}\sum_{j=-\infty}^{\infty}\sum_{L=-\infty}^{\infty}\int_{-\infty}^{\infty}\int_{-\infty}^{\infty} \times U(j,\omega)\,V(k-j-L,\omega-q)\,U_\phi(L,q)\,e^{ik\lambda}\,dw\,dq. \quad (7)$$

Thus eq. (6) may be written as

$$\frac{\partial \bar{E}(\lambda, t)}{\partial t} = -\sum_{k=-\infty}^{\infty}\sum_{j=-\infty}^{\infty}\sum_{L=-\infty}^{\infty}\int_{-\infty}^{\infty}\int_{-\infty}^{\infty}\left\{\frac{1}{a\cos\phi} \times U(j,\omega)\,U(k-j-L,-\omega-q)\,U_\lambda(L,q)\right.$$
(UX)

$$+\frac{1}{a\cos\phi}U(j,\omega)\,V(k-j-L,-\omega-q)\,V_\lambda(L,q)$$
(VX)

$$+\frac{1}{a}V(k-j-L,-\omega-q)\,U(j,\omega)\,U_\phi(L,q)$$
(UY)

$$+\frac{1}{a}V(k-j-L,-\omega-q)\,V(j,\omega)\,V_\phi(L,q)$$
(VY)

$$+W(j,\omega)\,[U(k-j-L,-\omega-q)\,U_p(L,q) + V(k-j-L,-\omega-q)\,V_p(L,q)]\left.\vphantom{\frac{1}{a}}\right\}e^{ik\lambda}\,d\omega dq$$
(W1)

$$+\sum_{k=-\infty}^{\infty}\sum_{j=-\infty}^{\infty}\int_{-\infty}^{\infty}\{f[U(j,\omega)\,V_a(k-j,-\omega) - V(j,\omega)\,U_a(k-j,-\omega)]$$
(CF)

$$+[U(j,\omega)F_1(k-j,-\omega) + V(j,\omega)F_2(k-j,-\omega)] \Big\} e^{ik\lambda}\,d\omega. \quad (8)$$
$$\text{(R1)}$$

The terms UX, VX, and UY and VY are the contributions of the non-linear wave interaction to the balance of the mean kinetic energy. UX and VX are the non-linear interactions associated with the longitudinal gradients of the zonal and meridional velocity. UY and VY are the non-linear interactions associated with the meridional gradients of the zonal and meridional velocity. The terms CF represent the effect of the deviation of velocity from geostrophy. The term R1 is the contribution of the Reynolds and molecular stresses. The terms in eq. (8) that involve vertical motions, the term W1, the linear effects of CF and R1 are not considered in the present analysis. The subscripts λ, ϕ and p denote partial differentiation with respect to longitude, latitude, and pressure, respectively.

7. Characteristics of non-linear interaction terms at 200 mb

The distributions of the non-linear interaction terms in the kinetic energy equation (8) have been computed for the region from 20° N to 85° N. For the calculation of non-linear interaction terms, a total of 28^3 interactions among 28 domains as shown in Tables 1 and 2 have to be computed. As discussed in the previous sections, we have found that the medium scale westerly waves with medium frequency $(k_m, -n_m)$ play an important role in the mid-latitudes. To gain an insight into the balance of kinetic energy of the medium scale westerly waves with medium frequency in wave number-frequency domains, the kinetic energy which is sizable is considered. Table 3 shows the maximum and minimum values of the non-linear interaction contributions from medium scale westerly waves with medium frequency due to the longitudinal and latitudinal convergence of the flux of kinetic energy (UX, VX, UY, VY).

It can be seen from Table 3 that the orders of magnitude of the non-linear interaction terms corresponding to the longitudinal convergence of the flux of kinetic energy (UX, VX) are generally larger than that of the terms involving the meridional convergence of the flux of kinetic energy (UY, VY). The regional distributions of the non-linear interaction terms (UX, VX) are specifically shown in Fig. 7. In Fig. 7a for term UX, the regions over the Eurasian continent attain large positive values, whereas negative minimum values are located over the North Atlantic. Fig. 7b shows that the negative minimum values of the term VX prevail over the North Pacific, whereas positive maximum values are located south of negative values. It is found from Fig. 7 that the primary non-linear interactions occur at latitudes between 30° N and 50° N. The non-linear interaction contributions are elongated along the latitude circle. This indicates that the longitudinal convergence of the flux of kinetic energy along the latitude circle between 30° N and 50° N is relatively important.

Table 3. *Maximum and minimum values of non-linear interaction contributions* $(k_m, -n_m)(K', N')(K'', N'')$; K' and K'' are composed of all wave numbers. N' and N'' *are composed of all frequencies*

	UX	VX	UY	VY
Maximum	10.9	10.9	2.9	0.17
Minimum	−2.9	−19.5	−2.7	−0.28

Units: 10^{-4} m^2 s^{-3}.

In order to identify the relatively important waves embedded in the non-linear interaction for regional contributions, we divide the wave number K and frequency N in (K', N') (K'', N'') into particular domains as shown in Tables 1 and 2. Figs. 8a, b show the regional distributions of the non-linear interaction $(k_m, -n_m)$ $(k_L, 0)$ $(k_m, -n_m)$ due to the terms UX and VX, respectively. We found that the results for the distributions of the non-linear interaction contributions in Fig. 8 were quite similar to those in Fig. 7. Comparison between the distributions in Figs. 7 and 8 indicates that the interaction between $(k_L, 0)$ and $(k_m, -n_m)$ is a primary contribution of non-linear interactions to the balance of the kinetic energy of waves $(k_m, -n_m)$ i.e. medium scale westerly waves with medium frequency.

8. Characteristics of non-linear interaction terms at 500 mb

In order to examine the structure and regional behavior of non-linear interactions at the various

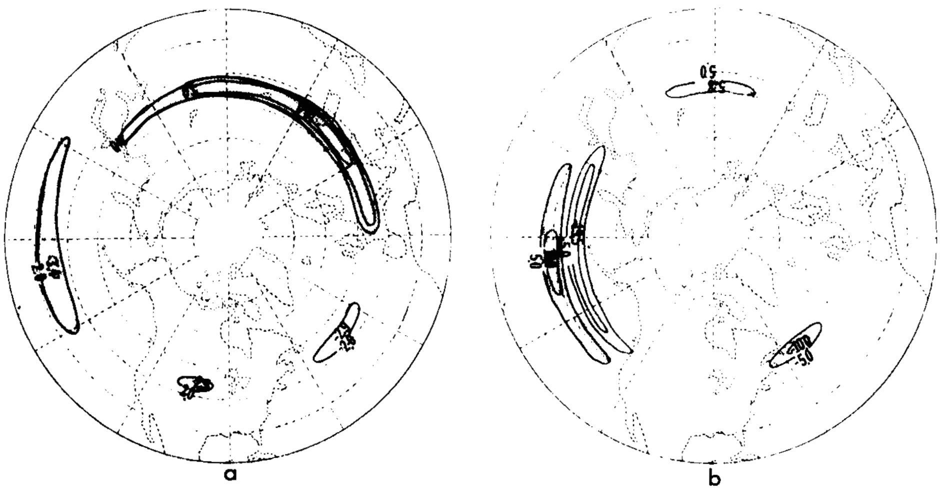

Fig. 7. Regional contributions of the non-linear interactions $(K_m, -n_m)$ (K', N') (K'', N'') at 200 mb (units 10^{-4} m^2 s^{-3}). (a) Term UX; (b) term VX. For the sake of clarity, the zero contour is not plotted. Dotted areas represent positive contributions from non-linear interactions.

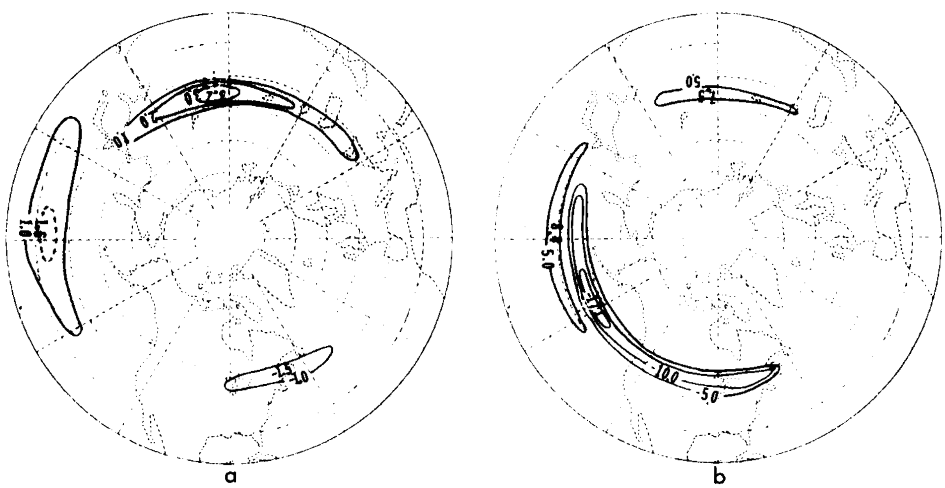

Fig. 8. As in Fig. 7 except for the non-linear interactions $(K_m, -n_m)$ $(K_L, 0)$ $(K_m, -n_m)$ at 200 mb. (a) Term UX; (b) term VX.

pressure levels, we analyze the data at 500 mb. Figs. 9a, b show the distributions of the non-linear interactions $(k_m, -n_m)$ (K', N') (K'', N'') for the terms UX and VX, respectively. It is found in Fig. 9a that the non-linear interaction involving the longitudinal convergence gives positive contributions over the regions of central Europe and the east coast of Asia, whereas over the region of the North Atlantic there is a negative contribution. The elongated positive contributions around 50° N over the regions of the east coast of Asia, the North Pacific, and North America are clearly seen in Fig. 9b with maximum contribution over western North America. It should be noted that at 200 mb over the region of the North Pacific, the contribution is negative (Fig. 7b).

Similarly, we have found that the non-linear interactions $(k_m, -n_m)$ $(k_L, 0)$ $(k_m, -n_m)$ for the terms UX and VX contribute substantially to the balance of kinetic energy of medium-scale westerly waves with medium frequency (Fig. 10). The large negative values are generally in the region of the east coast of Asia. It is seen from Figs. 8 and 10 that the maximum kinetic energy of the waves (k_m, $-n_m$) in the Pacific as shown in Figs. 3b and 2b is characterized by a positive contribution (supply spectral energy) from non-linear interactions. We also have found that the regions at 200 mb in Fig. 8b (at 500 mb in Fig. 10b) located to the north (south) of the maximum intensity of kinetic energy over the Pacific (Fig. 3b at 200 mb, Fig. 2b at 500 mb) are characterized by negative values (extracted spectral energy by non-linear interactions).

We conclude that the locations of maximum kinetic energy of the waves (k_m, $-n_m$) over the Pacific region correspond closely to the locations of positive contributions from non-linear interactions. This indicates that the non-linear interactions play an important rôle in the dynamics of atmospheric waves, which has also been found by others (Kao and Lee, 1977; Tsay and Kao, 1978; Kao and Chi, 1978).

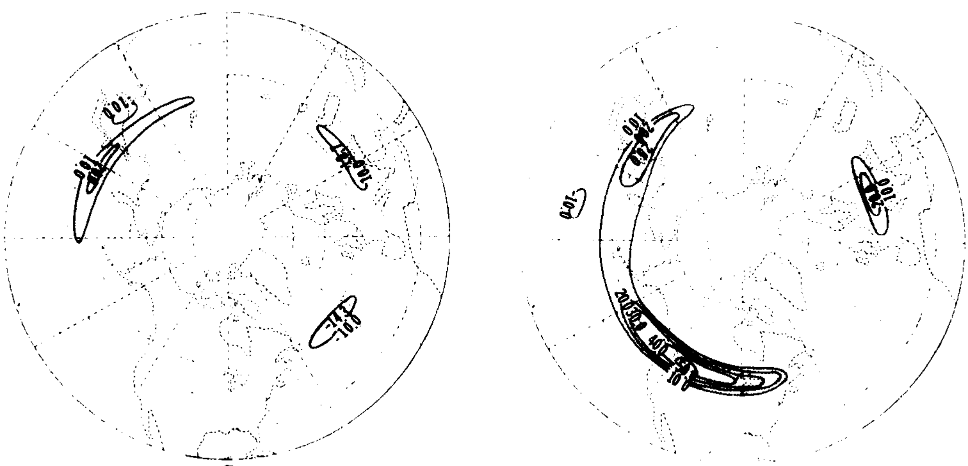

Fig. 9. As in Fig. 7 except at 500 mb. (a) Term UX; (b) term VX.

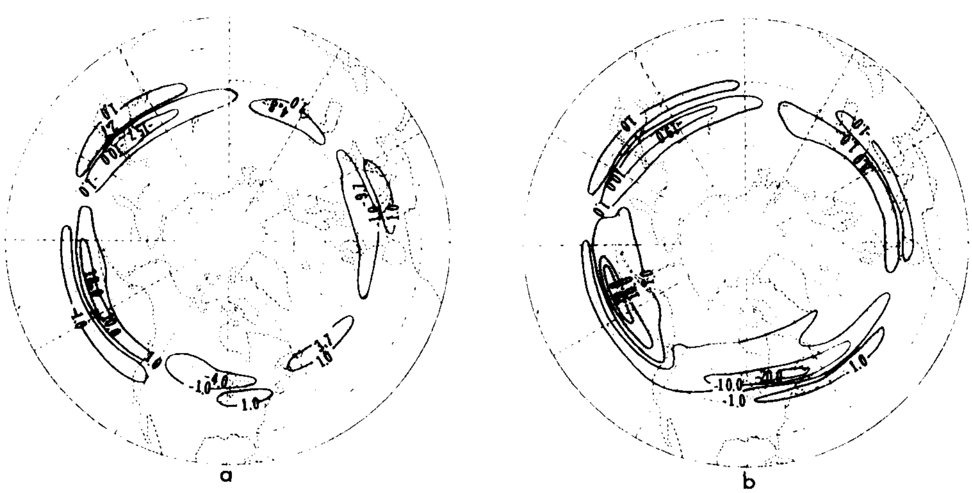

Fig. 10. As in Fig. 8 except at 500 mb. (a) Term UX; (b) term VX.

9. Conclusions and discussion

The regional distributions of kinetic energy have been computed using Fourier transform techniques in a wave number-frequency domain for the pressure levels of 850 mb, 500 mb and 200 mb. The distribution of kinetic energy showed a strong geographical dependence. At 500 mb it was found that the westerly waves with low frequency made contributions at the east coast of Asia and north of central Europe. The easterly waves with low frequency gave contributions to kinetic energy east of the North Pacific and over the North Atlantic. Fig. 1d showed that the maximum intensities of kinetic energy located over the North Pacific and the East Coast of North America were dominated by westerly waves with medium frequency. In view of the fact that the waves with medium frequency have been recognized as giving substantial contributions in mid-latitudes, we have concentrated our analysis on waves with medium frequency. It was found that medium scale waves with medium frequency made significant contributions, which was consistent with the geopotential height analyses of Blackmon (1976). We also found that the westerly waves embedded in the medium scale waves with medium frequency were apparently responsible for the 2 distinctive maxima located over the North Pacific and the east coast of North America.

In order to analyze the effects of the non-linear interactions on the regional distribution and characteristics of the kinetic energy of the medium scale westerly waves with medium frequency, the time-mean kinetic energy equation of the motion was examined. We found that the order of magnitude of the non-linear interactions corresponding to the longitudinal convergence of the flux of kinetic energy was generally larger than that of the terms involving the meridional convergence of the flux of kinetic energy. The primary non-linear interactions occurred at mid-latitudes between 30° N and 50° N and were elongated along the latitude circles. The regions at 200 mb (500 mb) located to the north (south) of the maximum intensity of kinetic energy over the North Pacific were characterized by a negative contribution from non-linear interactions. Our analysis has shown that the distribution of maximum kinetic energy of atmospheric waves in the region of the North Pacific is positively correlated with the distribution of the non-linear interaction contribution. It indicated that the non-linear interactions played an important röle in the dynamics of atmospheric waves.

10. Acknowledgement

Professor S. K. Kao died while this work was being carried out. Dr. Lee and Mr. Zhao dedicate it to the memory of a man with a unique affection. This work was supported by the U.S. National Aeronautics and Space Administration under Contract NAS-5-25373.

REFERENCES

Blackmon, M. L. 1976. A climatological spectral study of the 500 mb geopotential height of the northern hemisphere. *J. Atmos. Sci. 33*, 1607–1622.

Blackmon, M. L., Wallace, J. M., Lau, N. C. and Mullen, S. L. 1977. An observational study of the northern hemisphere wintertime circulation. *J. Atmos. Sci. 34*, 1040–1053.

Blackmon, M. L., Madden, R. A., Wallace, J. M. and Gutzler, D. S. 1979. Geographical variations in the vertical structure of geopotential height fluctuations. *J. Atmos. Sci. 36*, 2450–2466.

Blackmon, M. L. and Lau, N. C. 1980. Regional characteristics of the northern hemisphere wintertime circulation: a comparison of the simulation of a GFDL general circulation model with observations. *J. Atmos. Sci. 37*, 497–514.

Burrows, W. R. 1976. A diagnostic study of atmospheric spectral kinetic energetics. *J. Atmos. Sci. 33*, 2308–2321.

Gruber, A. 1975. The wave number-frequency spectra of the 200 mb wind field in the tropics. *J. Atmos. Sci. 32*, 1615–1625.

Kao, S. K. 1968. Governing equations and spectra for atmospheric motion and transports in frequency wave number space. *J. Atmos. Sci. 25*, 32–38.

Kao, S. K. 1980. Equations of kinetic and available potential energy evaluation in wave number frequency space. *Pure and Appl. Geophys. 118*, 867–879.

Kao, S. K. and Chi, C. N. 1978. Mechanism for the growth and decay of long- and synoptic scale waves in the mid-troposphere. *J. Atmos. Sci. 35*, 1375–1387.

Kao, S. K. and Lee, H. N. 1977. The non-linear interactions and maintenance of the large-scale moving waves in the atmosphere. *J. Atmos. Sci. 34*, 471–485.

Kao, S. K. and Taylor, V. R. 1964. Mean kinetic energies of eddy and mean currents in the atmosphere. *J. Geophys. Res. 69*, 1037–1049.

Kao, S. K. and Wendell, L. L. 1970. The kinetic energy of the large-scale atmospheric motion in wave number-frequency space (I). Northern hemisphere. *J. Atmos. Sci. 27*, 359–375.

Lau, N. C. 1978. On the three-dimensional structure of the observed transient eddy statistics of the northern hemisphere wintertime circulation. *J. Atmos. Sci. 35*, 1900–1923.

Lau, N. C. 1979. The structure and energetics of transient disturbances in the northern hemisphere wintertime circulation. *J. Atmos. Sci. 36*, 982–995.

Steinberg, H. L., Wiin-Nielsen, A. and Yang, C. H. 1971. On non-linear cascades in large-scale atmospheric flow. *J. Geophys. Res. 76*, 8629–8640.

Tenenbaum, J. 1976. Spectral and spatial energetics of the GISS model atmosphere. *Mon. Wea. Rev. 104*, 15–30.

Tsay, C. Y. and Kao, S. K. 1978. Linear and non-linear contributions to the growth and decay of the large-scale atmospheric waves and jet stream. *Tellus 30*, 1–14.

Wendell, L. L. 1969. A study of the large-scale atmospheric turbulent kinetic energy in wave number-frequency space. *Tellus 21*, 760–788.

Wiin-Nielsen, A. 1967. On the annual variation and spectral distribution of atmospheric energy. *Tellus 19*, 549–559.